International Journal of Engineering & Technology, 7 (4.20) (2018) 588-593

SPC

International Journal of Engineering & Technology

Website: www.sciencepubco.com/index.php/IJET

Research paper

Experimental and Numerical Modeling of DNAPL Mass Discharge from the Elliptic Pool in Saturated Homogeneous Sandy Soil

Hatem Asal Gzar[1], Rasha Abdulwahed Hussain[2]

[1,2] Civil Engineering Department, College of Engineering, Wasit University, Iraq.
**Corresponding author E-mail: hatam_asal@yahoo.com*

Abstract

"The present study aims to study the dissolution and mass transport of trichloroethylene (TCE) as Dense Non Aqueous Phase Liquid (DNAPL) in saturated porous media." A rectangular Perspex tank of internal dimensions (150cm length 20cm width and 40 cm height) used to represent the model aquifer. The tank was packed with homogenous soil (Karbala sand)"."Unidirectional flow at five different interstitial velocities (0.9, 1.8, 2.34, 2.7, and 3.6) cm/hr assumed to study the process. The average mass transfer coefficient" was determined for each velocity .Their values were increased with increasing the velocity reaching a limit value" .A conservative tracer is used to obtain the longitudinal and transverse aquifer dispersivities"."An elliptic shape of (TCE) pool was used to carry out the dissolution processes. Steady state dissolved (TCE) concentrations at downstream were collected from ten ports with two different depths under five interstitial velocities". Two linear relationships are created from an elliptic trichloroethylene pool: these relationships were between the average Peclet number in x-direction ($Pe^*_{x(e)}$) with the overall Sherwood number ($Sh^*_{(e)}$), and the other between the average Peclet number in y-direction ($Pe^*_{y(e)}$) with the overall Sherwood number ($Sh^*_{(e)}$)". A numerical modeling was achieved using **COMSOL** software.

Keywords: *Dissolution; Homogeneous soil; Mass transport; Numerical modeling ;TCE pool*

1.Introduction

Natural subsurface water system contamination by Non-Aqueous Phase Liquids (NAPLs), has taken a wide attention by numerous environmental scientists and engineers. Petroleum hydrocarbons and organic solvents are the most NAPLs ,the main causes of these liquids reaching to the subsurface formation are by leakage from underground storage tanks, landfills of hazardous waste, disposal sites, pipelines ruptured , leaching from recycled wastes, and surface spills. Chlorinated solvent like trichloroethylene (TCE) and tetrachloroethene (PCE) are widely used in different industrial actions. After the spilling of NAPL, it migrates to the subsurface environment by the vadosezone, part of it may be confined and restrained within the (unsaturated porous formation) in the shape of ganglia or pools, that are no more time takes to get in touch with the main body of (NAPL). The entrapped NAPLS both pools and ganglia would be a continuous ground water contamination source because of their low solubilities and slow dissolution rates within the ground water [1].

When NAPLs reaching the water table, the compounds that have densities more than water, which called sinkers (chlorinated solvents); gives pressure head at the capillary fringe is large enough, continuing in downward migrate and leaving trapped ganglia until they touch the solid layer (impermeable layer), where small cross section pools (a flat source zone) would stars form [2], while NAPLS compound that have densities lighter than of water "floaters, e.g., Petroleum products" would spread laterally when they reach the saturated region, forming a pool floating on the water table [3]. In case of the inclined impermeable layer the sinker pools would migrate along the formation; but the floater pools would move in the declining hydraulic gradient direction. When the pollution occurs; many dangers substances transports through the ground water entering the food, water chain and finally harm human directly or indirectly [4,5].

A large number of computers, experimental and also theoretical studies have concentrated on the both ganglia dissolution [6,7,8] and the pools dissolution [9,10,11,12,13]. On the ground- water the dissolved concentration of NAPL is mostly controlled by the processes of mass transfer interface which are rate limited and slow [14,15]. The NAPL dissolves to the aqueous phase through the physical contact with the ground -water. The"solubility" of the organic materials represents the equilibrium concentration of these materials in water at a certain temperature and pressure. For all practical objectives, the maximum concentration of that material in water represents the solubility [16].

The"experimental and numerical studies"that focused on the dissolution process of NAPL in three dimensions are very limited [5,17,18,19,20,and 21].The present study focused on the dissolution of trichlororethylene as (DNAPL) in three dimensional saturated" homogeneous, and isotropic porous medium".

2. Material and Methods

Tap water was used in the experiments, the biological growth in the experimental aquifer was prevented by adding sodium azide 200 (mg/l) to thewater storage tank (water source). Trichloroethylene is used as Dense Nonaqueous Phase Liquid.

2.1. Porous Medium Characterization

The porous medium that used in the present study was Karblalaa 's sand which is a sand obtained from Karblaa 's Governorate lands south of Iraq. The used sand was passing through 1mm mesh. Tests such as particle size distribution and porosity were performed on Karblaa's sand.

2.2 Particle size Distribution

Mechanical sieve analysis was used to obtain the particle size distribution as shown in Fig (1).The range of grain sizes was indicated by the coefficient of uniformity (Cu), this coefficient was (2.21).The dry sand bulk density and porosity were 1.6 g/cm3 and 0.312 respectively.

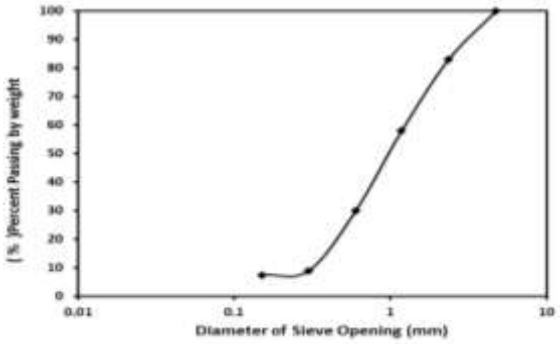

Fig 1: Particle size distribution curve of Karblaa's sand

3. Experimental Aquifer Setup

Three dimensions bench scale laboratory aquifer was used in the present study to carry out the dissolution experiment as shown in Fig(2a) and Fig (2b) The internal dimensions of the tank are (150cm×20cm×40cm) length ,width , and height respectively. The tank was made of 1cm thick Perspex plate. The tank contains" three chambers: the middle chamber which filled with sand and the two other chambers are 10 cm away from the both sides of the tank" (the side chambers are represent clear wells) ,the clear wells are filled with water, maintaining constant heads, and separated from the middle chamber by two perforated Perspex plates covered with a filtration cloth to "prevent the sand passing to the side chambers". A peristaltic pump was used to control the flow rate through the model aquifer**,** and the tap water was pumped from 60 liters storage tank to the influent clear well by 0.5cm inner diameter tube. The effluent clear well is connecting also by 0.5 inner diameter tube to a valve and 8 liters constant head tank to achieve the outflow rate**.**

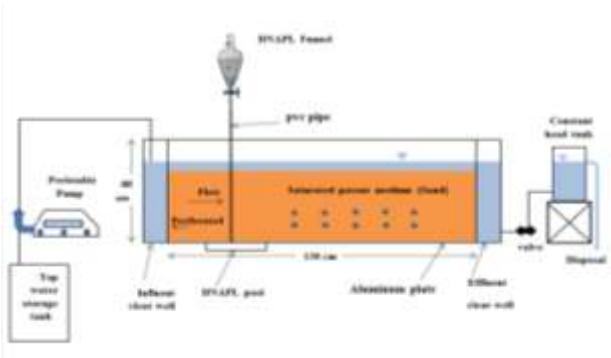

Fig 2 a: Schematic diagram of the bench-scale laboratory aquifer

Fig 2 b: A picture of the laboratory aquifer.

3.1. DNAPL Pool Formation and Aquifer Packing

A flat DNAPL pool formation with the pool water interface is a significant key to this experimental design. The preceding work by [17] producing significant details about the formation of DNAPL pool and dissolution with bench scale laboratory aquifer". The DNAPL pool represented by 5cm deep perspex elliptic pan padded with aluminum sheet to avoid the corrosion, the ellipse pan is 15 cm (the major axis) and 10 cm(the minor axis), the cause behind the using of this pool shape is it represent the closest shape to the actual pool.7This pan was filled with a layer of sand and other of gravel and it covered with stainless steel mesh'. "The DNAPL (TCE) was injected to the pan from the bottom face by horizontally (0.3 cm)PVC tube connected to 500 ml conical funnel which contain a valve to control the flow rate" . In the upper half of the perspex pan the residual (DNAPL ganglia formation) can form when the injected DNAPL move the water from the gravel and sand layers within the pan. An aluminum plate is used at the bottom of the aquifer in order to prevent the corrosion, the plate dimensions are (130 cm length, 20 cm width and 0.3 cm thickness)."An elliptic disk with (15cm length and 10 cm width) was removed from the aluminum plate to confine the Perspex experimental pool.

4. Tracer analysis Test

The most common system which used to determine the dispersion coefficient represent by the tracer transport analysis, the tracer using is brine solution . Conductivity and resistivity are used to determine the tracer concentration [20]. The longitudinal dispersion coefficient values in the sand tank were found by the tracer transport experiment, and according the longitudinal coefficient the lateral and vertical dispersion coefficient were obtained to measure the concentration in three dimensions . An initial concentration of (1000 mg/l) of sodium chloride is used. The tracer transport is performed by injecting a solution of sodium chloride continuously under five different water velocities (0.9, 1.8, 2.34, 2.7, and 3.6) cm/hr. The observation points of the breakthrough data is recorded continuously 40 cm from the injected tracer. A portable ohmmeter probe employing to measure the concentration. The probe is fixed at the top of the tank at a depth of 3cm of the observation point in the saturated sand. The concentration is obtained according to the measured resistance by the ohmmeter. Samples of known concentration used to calibrate the measured resistance , for this reason a calibration curve was prepared.

5. Dissolution experiments

In the Perspex front face of the aquifer model ten ports (A-J) were made (Figure.3), five of them at 3cm and the rest on the 6 cm from the base of the aquifer. Ten points were used to draw the samples. All the sampling points located at 10 cm in the y-

direction of the aquifer (in the center line) to study the concentration distribution in the x-direction at the two depths mentioned. In addition to that in the centerline of the plume the maximum concentrations are form. In the direction of flow (longitudinal direction) the dispersion coefficient is more than it in the vertical and transverse directions. Five different interstitial velocities (0.9,1.8, 2.34,2.7, and 3.6) cm/h were used in this study to implement the dissolution experiment. 10-guaged stainless with steel needles "manufactured by Sherwood Medical, St. Louis, MO, USA" was inserted into the porous medium by pushing them in the ports in order to collect the samples, and to forbid the needles clogging a wire inserted inside them during the process of the placement. Ten dissolution experiments were done (five in each depth); five selected points at each depth at the downstream of DNAPL pool and at a certain interstitial velocity . The first sampling group coordinates are (15,10,3), (30,10,3), (45,10,3),(60,10,3), and (75,10,3) , respectively at 3 cm depth from the pool surface. The second sampling group coordinates: (15,10,6), (30,10,6),(45,10,6),(60,10,6),and (75,10,6), respectively at 6 cm depth from the pool surface. The range of the flow rate was from 3 to 12 ml/min, these yield the velocities (0.9 - 3.6 cm/hr). The experimental conditions were at a temperature of 27 ◦C.

6."Samples collection and analysis"

When the steady state concentrations are obtained at the farthest port (J) from the DNAPL pool, the aqueous phase DNAPL is collected. The syringe volume with 5 ml is used to collect the interstitial water from the port points. From each location 1ml sample is obtained and saved in a glass vial. 200 samples were collected from the five ports in the sand at 3cm depth and 200 other samples collected at 6cm from the top of the pool. The ten samples collected every 24 hours. The analysis of the samples was by"Gas Chromatograph(Shimadzu2010,Japan) equipped with flame ionization detector" (FID).

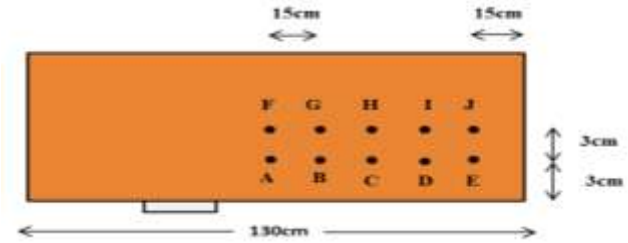

Fig 3: Sketch illustrate the sampling point locations within the saturated sand.

7."Transport Model"

The contaminant transport of the NAPL pool in the saturated homogeneous porous medium in three*dimensions,*under steady-state uniform flow conditions, the dissolved organic, non-decaying, and sorption occurring under local equilibrium conditions; is defined by the following equation "[5,22]:

$$D_x \frac{\partial^2 C(t,x,y,z)}{\partial x^2} + D_y \frac{\partial^2 C(t,x,y,z)}{\partial y^2} + D_z \frac{\partial^2 C(t,x,y,z)}{\partial z^2} - V_x \frac{\partial C(t,x,y,z)}{\partial x} = R_f \frac{\partial C(t,x,y,z)}{\partial t} \quad (1)$$

Where: D_x, D_y, and D_z are the longitudinal, lateral, and vertical hydrodynamic dispersion coefficients respectively, V_x is the average unidirectional interstitial velocity of water; R_f is the retardation factor (dimensionless) and it value was 1.52 obtained by the following equation:

$$R_f = 1 + \frac{\rho_b K_d}{n} \quad (2)$$

Where: n : porosity, Kd: soil distribution coefficient ,ρ b :soil bulk density(g/cm3).

8.Model Parameters Estimation

8.1 Interstitial velocity

The following equation describes the determination of "interstitial velocity" within the sand model aquifer [23]:

$$V_x = \frac{Q}{hwn} \quad (3)$$

Where: Q is the volumetric flow rate of water, h is the water head ,w is the aquifer width, and n is the porosity of sand. Five interstitial velocities were used in the present study (0.9,1.8,2.34,2.7,and 3.6) cm/h.

8.2Hydrodynamic Dispersion Coefficients

The tracer transport test was used to determine thelongitudinaldispersion coefficient as mentioned previously, by using relative concentration (C/C◦) versus the time on arithmetic probability paper (the graphical technique) as [5]:

$$D_x = 0.5\left[\frac{t_{84} - t_{16}}{2t_{50}}\right]V_x \quad (4)$$

where t_{84}, t_{16} , and t_{50} are the" times corresponding to3 (C/C◦) ratios of 84%",16%, and 50% respectively. The final hydrodynamic longitudinal dispersion coefficient is "equal to the summation of dispersive flux" which resulted from the equation (3) and diffusive flux which resulted from multiplying the dispersion coefficient of TCE ($8.4*10^{-6}$) cm^2/s by the sand tortuosity 1.43 [5].The lateral dispersion coefficient D_y are used as "0.1 of the longitudinal dispersion coefficient" and "the vertical dispersion coefficient is equal to the lateral dispersion coefficient".

9. The Numerical Modeling.

A numerical solution using (**Comsol** Multiphysics Software**v5.3a**) employed in the present study to solve the advection-dispersion - mass transport equation in a three dimensional model in saturated isotropic-homogenous sandy soil and uniform flow. Fig (3,4) shows the geometry of the model and mesh details respectievely. The number of Tetrahedral is 74801,the mesh settings were represented by : sequence type of physics –controlled mesh and the element size is extremely fine which is the most precision using by this software .The input parameters are shown in table (1).

Table 1: Input parameters of numerical modeling

Parameter	Value	Unit
L,H,b	1.3,0.31,0.2	m
Cs	1100	mg/l
Dx,Dy,Dz	(0.3-1.01),(0.03-0.101)	cm2/h
n	0.312	Dimensionless
ρ	1.6	gm/cm3
V_x	(0.9,1.8,2.34,2.7,and,3.6)	cm/h
R_f	1.52	Dimensionless

The "initial and boundary conditions for circular–elliptic shaped NAPL pool are:

$$C(0, x, y, z) = 0 \quad (5)$$

$$C(t, \mp\infty, y, z) = 0 \quad (6)$$

$$C(t, x, y, 0) = C_s \qquad x, y \in R_{(e)} \quad (7)$$

$$\frac{\partial C(t, x, y, 0)}{\partial z} = 0 \qquad x, y \notin R_{(e)} \quad (8)$$

$$C(t, x, y, \infty) = 0 \quad (9)$$

C_s is the solubility concentration of DNAPL for trichloroethylene is 1100 mg/l, and $R_{(e)}$ is the elliptic DNAPL-water interfacial area as:

$$\frac{\left(x-l_{x_o}\right)^2}{a^2} + \frac{\left(y-l_{y_o}\right)^2}{b^2} \geq 1$$

Where: a, b are the major and minor semiaxes respectively, which center located at $x= l_{x_o}$,$y=l_{y_o}$.

These conditions were represented numerically by: no flux at all the boundaries of the geometry at time equal to zero,the concentration equal zero at any point at time equal to zero(initial values), the concentration is equal to 1100 mg/l at z=0 (in the elliptic pool), the inflow of water at the first boundary with zero concentration, and the outflow at the last boundary.

10. Results and Discussion

Figures (5) to (9) show a comparison of the calculated and measured trichloroethylene (TCE) concentration with time 8days downstream of the pool at two distances (15,and 75) cm and two depths (3 cm, 6 cm) above the pool surface under five interstitial velocities (0.9, 1.8, 2.34, 2.7,and 3.6) cm/h.

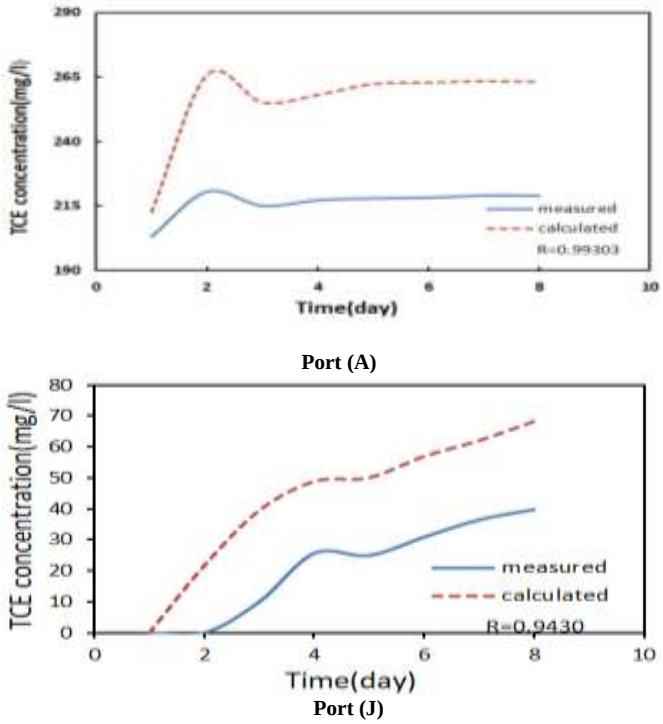

Fig 5: TCE concentration with time at the(first port (A) at Z=3cm), and the (end port (J) at Z= 6cm) at v=0.9 cm/h.

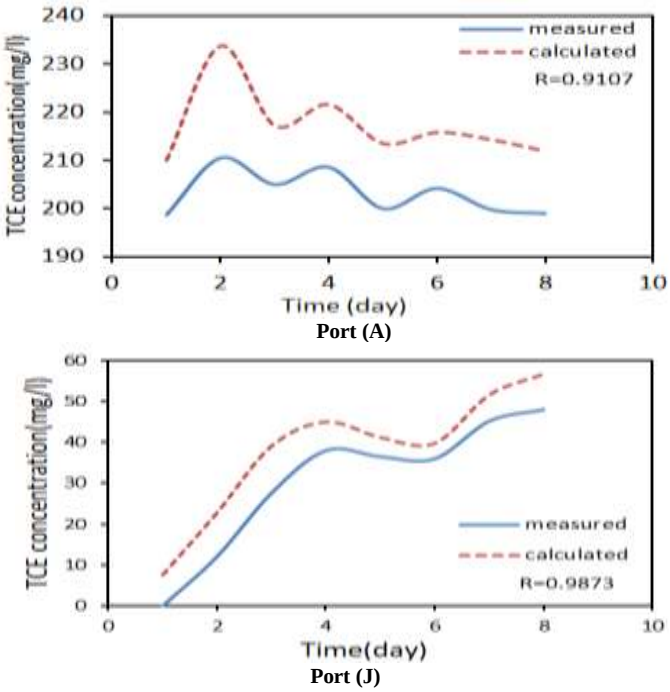

Fig 6: TCE concentration with time at the(first port (A) at Z= 3cm), and the (end port (J) at Z= 6cm) at v=1.8 cm/h.

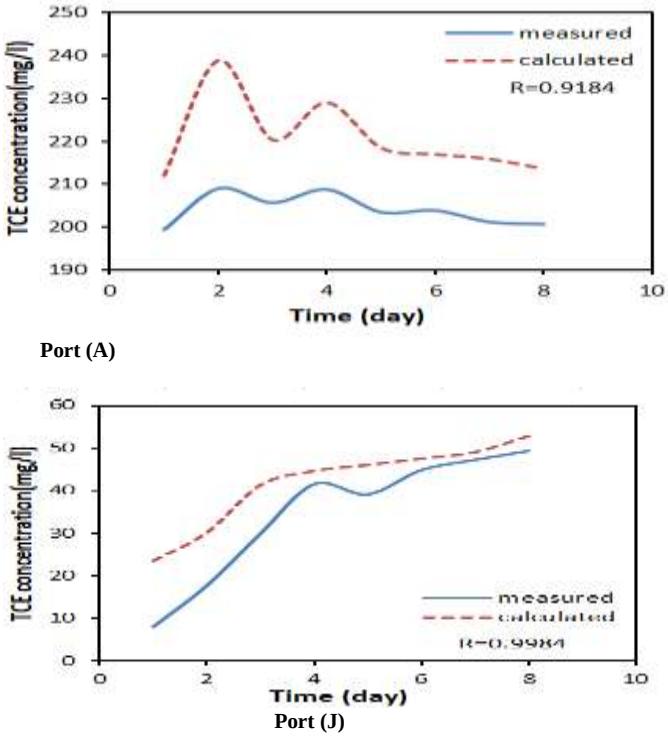

Fig 7: TCE concentration with time at the(first port (A) at Z=3cm), and the (end port (J) at Z= 6cm) at v=2.34 cm/h.

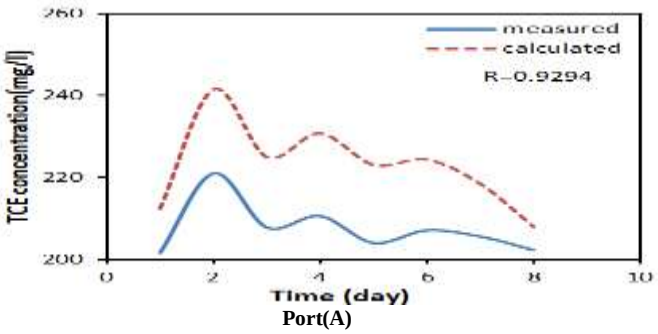

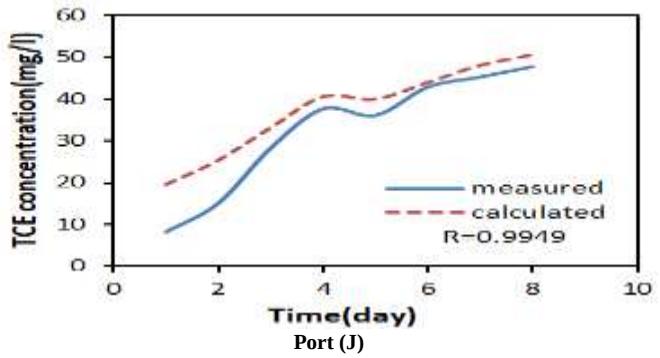

Fig 8: TCE concentration with time at the(first port (A) at Z=3cm), and the (end port (J) at Z= 6cm) at v=2.7 cm/h.

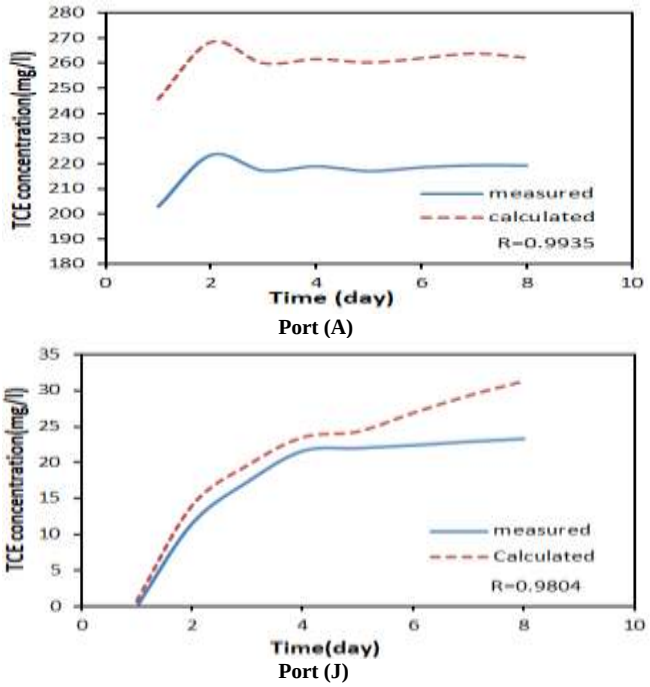

Fig 9: TCE concentration with time at the(first port (A) at Z=3cm), and the (end port (J) at Z= 6cm) at v=3.6 cm/h .

The present study shows that the maximum concentration observed at A(15,10,3) the nearest point to the TCE pool but the minimum concentration observed at J(75,10,6) the farthest point from the pool. TCE concentration observed over 75 cm downstream of the pool for 8 days .TCE concentration was declined with the time but this declining was little at little velocities and (0.9,1.8,and 2.34) cm/h ,more high declining observed at the velocities of 2.7cm/h,and 3.6 cm/h. Port (A) shows the same behavior (declining wave shape) at interstitial velocities of (1.8, 2.34, and 2.7) cm/h this may relates to "results of pore scale geometry and large scale shapeirregularities". But this port shows another different behavior at (0.9 and 3.6) cm/h .Port (J) the farthest point from the TCE pool shows nearly the same behavior(increasing curve from zero) at all the velocities this behavior relates to the diffusion , but the minimum value of concentration were recorded at this point(23.3) mg/l at the eighth day .The measured and calculated results were not very close but they gave the same behavior .The cause of this difference in the experimental and numerical results belongs to use TCE solubility Cs (maximum concentration of trichloroethylene) of 1100 mg/l in the numerical model but in fact it not reach to the max. concentration because of "volatile ,cosolvents, temperature, Ph, dissolved inorganic compounds (salinity),and dissolved organic compound".

10.1."Mass transfer correlation"

The average mass transfer coefficient (K*) is computed experimentally at each interstitial velocity by using the following equation [5]:

$$k^{*} = n\sqrt{\frac{4D_z V_x}{\pi L}} \qquad (10)$$

Where: L is the length of interface (15 cm) . The values of the average mass transfer coefficient (k*) at each velocity and the vertical dispersion coefficient are shown in table (2) :

Table 2: Mass transfer coefficient values

V_x(cm/h)	k*	D_z
0.9	0.015	0.0300
1.8	0.029	0.0588
2.34	0.036	0.0684
2.7	0.042	0.0790
3.6	0.055	0.1010

The (K*) values proportionally to the interstitial velocity, the reason belong to that is the increase in velocity leads to increase the concentration gradient at the DNAPL-water interface. The dimensionless mass transfer behavior is epitomized in the modified Sherwood number (Sh^{*}) terms , $Sh^{*}= K^{*} \ell_{c(e)} / De$ as shown in figures (10,11) where the characteristic length ($\ell_{c(e)}$) used here is the square root of the pool area (21.7 cm), and De value is $2.12*10^{-2}$ cm^2/h. The average Peclet numbers ;Pe*x(e) ,Pe *y(e) that represent the advection-dispersion mass transfer in x,y direction for elliptic pool, respectively ;were obtained by using equations (11), (12), and (13):

$$Sh^{*}_{(e)} = \frac{k^{*} \ell_{c(e)}}{D_e} \qquad (11)$$

$$Pe^{*}_{x(e)} = \frac{V_x a}{D_x} \qquad (12)$$

$$Pe^{*}_{y(e)} = \frac{V_x b}{D_y} \qquad (13)$$

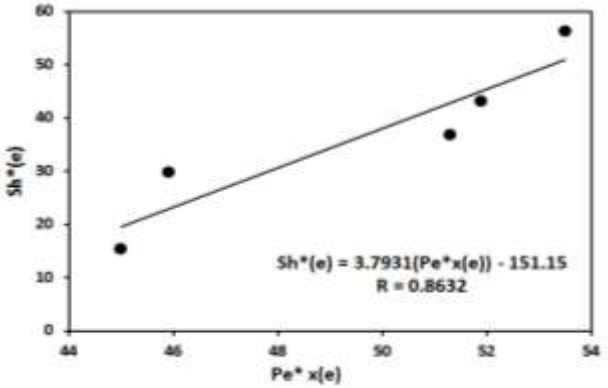

Fig 10: Sherwood number(Sh*) with Peclet number in x-direction Pe*x(e).

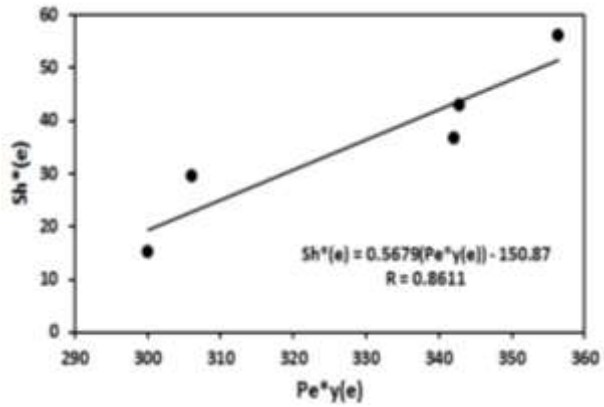

Fig11: Sherwood number(Sh ∗) with Peclet number in y-direction Pe∗y(e).

11. Conclusion

Theanalysis .of experimental. and numerical investigations.are gave the following conclusions. The concentration profile of TCE declines from port (A) and continue in declining with increasing (the time , the interstitial velocities , and the distance) reaching to port (J)." The time invariant average mass transfer coefficient is found at different interstitial velocities".The values of this coefficient are ranged from 0.015to 0.055cm/h". "It is increased proportionally with velocity toward a limiting value". Parameter .estimates for Pe∗x(e); Pe∗ y(e); Sh∗ (e) are .determined at different hydrodynamic conditions. The experimental and numerical results are not very close in their values but they had given the same behavior , and the regression between them are also presented here ranging (0.9107- 0.9984).

References

[1] Rubin, H., Narkis, N., & Carberry, J. (Eds.). (2013). Soil and aquifer pollution: non-aqueous phase liquids-contamination and reclamation. Springer Science & Business Media .

[2] Eberhardt, C., &Grathwohl, P. (2002). Time scales of organic contaminant dissolution from complex source zones: coal tar pools vs. blobs. Journal of Contaminant Hydrology, 59(1-2), 45-66..

[3] Parker, J. C., & Park, E. (2004). Modeling field-scale dense nonaqueous phase liquid dissolution kinetics in heterogeneous aquifers. Water Resources Research, 40(5).

[4] Sharma, J. K., Gautam, R. K., Nanekar, S. V., Weber, R., Singh, B. K., Singh, S. K., &Juwarkar, A. A. (2017). Advances and perspective in bioremediation of polychlorinated biphenyl-contaminated soils. Environmental Science and Pollution Research, 1-21

[5] Sulaymon, A. H., &Gzar, H. A. (2011). Experimental investigation and numerical modeling of light nonaqueous phase liquid dissolution and transport in a saturated zone of the soil. Journal of hazardous materials, 186(2-3), 1601-1614

[6] Seyedabbasi, M. A., Newell, C. J., Adamson, D. T., & Sale, T. C. (2012). Relative contribution of DNAPL dissolution and matrix diffusion to the long-term persistence of chlorinated solvent source zones. Journal of contaminant hydrology, 134, 69-81

[7] Christ, J. A., Ramsburg, C. A., Pennell, K. D., &Abriola, L. M. (2010). Predicting DNAPL mass discharge from pool-dominated source zones. Journal of contaminant hydrology, 114(1-4), 18-34..

[8] DiFilippo, E. L., &Brusseau, M. L. (2008). Relationship between mass-flux reduction and source-zone mass removal: analysis of field data. Journal of Contaminant Hydrology, 98(1-2), 22-35.

[9] Quinn, J., Geiger, C., Clausen, C., Brooks, K., Coon, C., O'Hara, S., ... &Holdsworth, T. (2005). Field demonstration of DNAPL dehalogenation using emulsified zero-valent iron. Environmental Science & Technology, 39(5), 1309-1318.

[10] Waldemer, R. H., Tratnyek, P. G., Johnson, R. L., &Nurmi, J. T. (2007). Oxidation of chlorinated ethenes by heat-activated persulfate: kinetics and products. Environmental Science & Technology, 41(3), 1010-1015.

[11] Chrysikopoulos, C. V., &Katzourakis, V. E. (2015). Colloid particle size-dependent dispersivity. Water Resources Research, 51(6), 4668-4683 .

[12] Essaid, H. I., Bekins, B. A., &Cozzarelli, I. M. (2015). Organic contaminant transport and fate in the subsurface: Evolution of knowledge and understanding. Water Resources Research, 51(7), 4861-4902.

[13] Christ, J. A., Ramsburg, C. A., Abriola, L. M., Pennell, K. D., &Löffler, F. E. (2004). Coupling aggressive mass removal with microbial reductive dechlorination for remediation of DNAPL source zones: a review and assessment. Environmental Health Perspectives, 113(4), 465-477.

[14] Logan, Bruce E. Environmental transport processes. John Wiley & Sons, 2012. [15] Sale, T. C., & McWhorter, D. B. (2001). Steady state mass transfer from single-component dense nonaqueous phase liquids in uniform flow fields. Water Resources Research, 37(2), 393-404.

[15] Zadeh, K. S., Shirmohammadi, A., Montas, H. J., & Felton, G. (2007). Evaluation of infiltration models in contaminated landscape. Journal of Environmental Science and Health Part A, 42(7), 983-988.

[16] Clement, T. P., Kim, Y. C., Gautam, T. R., & Lee, K. K. (2004). Experimental and numerical investigation of DNAPL dissolution processes in a laboratory aquifer model. Groundwater Monitoring & Remediation, 24(4), 88-96.

[17] Lee, K. Y., &Chrysikopoulos, C. V. (2006). Dissolution of a multicomponent DNAPL pool in an experimental aquifer. Journal of hazardous materials, 128(2-3), 218-226.

[18] [Wang, H., & Wu, H. (2009). Analytical solutions of three-dimensional contaminant transport in uniform flow field in porous media: A library. Frontiers of Environmental Science & Engineering in China, 3(1), 112-128.

[19] Cirpka, O. A., Olsson, Å., Ju, Q., Rahman, M. A., &Grathwohl, P. (2006). Determination of transverse dispersion coefficients from reactive plume lengths. Groundwater, 44(2), 212-221.

[20] Chen, K., Zhan, H., & Zhou, R. (2016). Subsurface solute transport with one-, two-, and three-dimensional arbitrary shape sources. Journal of contaminant hydrology, 190, 44-57.

[21] Chrysikopoulos, C. V., Hsuan, P. Y., Fyrillas, M. M., & Lee, K. Y. (2003). Mass transfer coefficient and concentration boundary layer thickness for a dissolving NAPL pool in porous media. Journal of hazardous materials, 97(1-3), 245-255.

[22] Jawitz, J. W., Fure, A. D., Demmy, G. G., Berglund, S., & Rao, P. S. C. (2005). Groundwater contaminant flux reduction resulting from nonaqueous phase liquid mass reduction. Water Resources Research, 41(10).